Nondestructive evaluation of the interface between ceramic coating and stainless steel by electromagnetic method

2016 IOP Conf. Ser.: Mater. Sci. Eng. 147 012030

(http://iopscience.iop.org/1757-899X/147/1/012030)

IOP Conf. Series: Materials Science and Engineering **147** (2016) 012030 doi:10.1088/1757-899X/147/1/012030

Nondestructive evaluation of the interface between ceramic coating and stainless steel by electromagnetic method

A Savin[1], R Steigmann[1], N Iftimie[1], F Novy[2], P Vizureanu[3], M L Craus[1,4] and S Fintova[5,6]

[1]National Institute of Research and Development for Technical Physics, Iasi, Romania
[2]University of Žilina, Žilina, Slovak Republic
[3]Technical University Gh.Asachi, Iasi, Romania
[4]Joint Institute for Nuclear Research, Dubna, Russia
[5]Institute of Physics of Materials AS CR v.v.i., Brno, Czech Republic
[6]Materials Research Centre, Brno University of Technology, Brno, Czech Republic

E-mail: asavin@phys-iasi.ro

Abstract. Protecting coatings as thermal barrier coating (TBC) are used for yield improvement of equipment working at high temperature. Zirconia doped with yttria ceramics are considered a good TBC material due of its low thermal conductivity, refractory, chemical inertness and compatible thermal expansion coefficient with metallic support. The paper proposes the use of an electromagnetic method for evaluation of coatings on stainless steel using a sensor with metamaterial lens and comparison of the results with those obtained by complementary methods.

1. Introduction

Protecting coatings as thermal barrier coating (TBC) are used for yield improvement of equipment working at high temperature. The most common application is the one of gas turbine or diesel engines, where TBC's are frequently used [1].

The electromagnetic methods for nondestructive testing (NDT) at high frequencies in the MHz range allow the characterization of the thin coating adhesion and testing for the detecting possibility to appear the defects between the coating and support materials. Other well-known NDT methods for emphasizing flaws/fatigue or stress are acoustic emission for cracks detection in TBCs [2]; infrared thermography to examine the delamination of TBC's [3]; piezo-spectroscopy measure stress levels and failure in TBCs by analysis of the shape of luminescence spectra [4]; impedance spectroscopy; electromagnetic methods, for characterization of the thin coating adhesion/presence of spallation; ultrasound methods, etc. The last decades, NDT techniques have been developed due to the miniaturization requirements as due to necessity to improve the properties of new and advanced materials used in the construction of devices/components of mechanical systems.

Zirconium oxide (ZrO_2) is an important versatile ceramic material due its novel physical-chemical properties [5], [6], most commonly used for TBC [7]. The mechanical functional properties of zirconia are associated with its tribological performance such as friction and wear. Furthermore, zirconia based ceramic components have excellent fracture toughness, very good wear resistance, high corrosion stability, low thermal conductivity and coefficient of thermal expansion in range of steel. All these

properties characterize zirconia as a leading structure material for highest wear stress in several application fields, even aircraft engines such as blades, guide-vanes, etc.

The system Y_2O_3–ZrO_2 has been extensively studied for more than 50 years [8], [9]. This work is focused on the properties of Yttria stabilized zirconia (YSZ) as part of TBC. Most present day YSZ is normally used for the TBC [10] due to its outstanding mechanical properties depending on the yttrium content. Stainless steels are very often used as support for TBC, the most widely used is AISI 316L. The AISI 316L steel is low carbon version of AISI 316 (≤0.03 %C), which may be susceptible to intergranular corrosion in certain corrosive media after it is welded or otherwise heated at temperatures between 430 and 860 °C.

This paper proposes to present an electromagnetic method for evaluation of zirconia coating (to differentiate the areas with good/inferior coating quality) on stainless steel using an electromagnetic methods based on the sensor with metamaterial (MM) lenses that assure an enhancement of spatial resolution. NDT method is very important, because the nanocomposites, in which nanometer-sized phase particles are dispersed within a ceramic matrix and/or at grain boundaries, have shown significant improvements in strength and creep resistance, even at high temperatures, and assure an exciting future different technological fields. The obtained results are compared with alternative methods of characterization such as Scanning Electron Microscopy (SEM), X-ray diffraction and metallography.

2. Experimental details. Materials

Zirconia is an important ceramic material with an increasing range of applications. Used as top-coating (is nonconductive and nonmagnetic) behaves like an air gap between conductive support and electromagnetic sensor. Ceramic materials based on zirconia have attracted attention due to their unique physical properties: high fracture toughness and bulk modulus, low thermal conductivity, extremely refractory, chemically inert, corrosion resistant, high dielectric constant.

TBC is a system which consists of a ceramic coating of low thermal conductivity such as zirconia deposited on metallic support using either plasma spraying or electron beam physical vapor deposition processes, with or without Thermally Grown Oxide (TGO), deposited on a metal support [11-13]. Theoretically, the weakest part of TBC is the substrate-ceramic interface, where fractures can appear under the action of thermal shock. Zirconia compositions can also have one weakness, their tendency to low temperature degradation in the presence of moisture. This is a kinetic phenomenon in which polycrystalline tetragonal (t) material slowly transforms to monoclinic (m) zirconia between room temperature and around 400 °C, depending on the stabilizer, its concentration, and the grain size of the ceramic. It is well known that three polymorphic forms of pure ZrO_2 can be found: the monoclinic state, $P2_1/c$, stable at temperatures below 1170 °C, the tetragonal phase, $P4_2/nmc$ stable in the temperature range between 1170-2370 °C and the cubic, Fm-3m phase, appearing at a temperature above 2370 °C [7], [14].

2.1. Studied samples

The use of YSZ ceramics quality of top coat applied to the surface of metallic surface increased, widely used as thermal protective layer dedicated metallic components in high temperature region on engines and gas turbines. They can enhance component reliability and increase the operating temperature, resulting in higher efficiency and better environmental benefits [15], [16]. Laminar structures of YSZ TBC layers deposited on stainless steels are typically porous and the pore size and character depends on the process parameters.

The AISI 316L used as support is austenitic stainless steel, having good corrosion resistance, (composition in wt. % according to EN 1.4404). After mechanical processes we obtain specimens with dimensions 20x80 mm^2 and 2 mm height. Electrical conductivity is 1.3513×10^6 $S \cdot m^{-1}$, thermal expansion coefficient 17.2×10^{-6} K^{-1} at 473 K, but may be susceptible to intergranular corrosion in certain corrosive media after it is welded or otherwise heated at high temperatures [17], [18]. Deposition of ceramic coatings was done using plasma torch F 400 with commercial atmospheric

equipment APS 100 produced by Swiss Company Plasma-Technik AG. The decrease in physical dimensions down to the nanometer scale is often linked with a dramatic change of the physical and electrochemical properties of materials. Grain boundaries are regarded as possessing high defect densities and/or enhanced mobility.

The transformation t→m during a cooling process is accompanied by a volume increase (approximately 4 %) and shear distortion, sufficient to cause failure. At nanoscale level, the main method of tetragonal phase stabilization is the introducing in zirconia lattice of the stabilization component such as Ce or Y. A crack growth approach has been connected for TBC with delamination and spallation. Monolithic coatings of various thickness consisting of zirconia doped with 20 % yttria and sandwich zirconia doped with 20 % yttria and pure yttria coatings were deposited on AISI 316L. The coating material is produced by Metco as powder Metco^{TM} 202NS and Metco 6035A-1 used for plasma spraying, having excellent resistance to oxidation and corrosion at temperature till 1000 °C and can create excellent thermal barrier coatings. Pure yttrium oxide is a highly stable compound with a high melting point and is very inert chemically and exhibits excellent electrical insulation (volume resistivity and dielectric breakdown strength).

2.2. Experimental setup

2.2.1 Electromagnetic sensor. The sensor is absolute send-receiver type and has the principle scheme given in figure 1a and physical realization in figure 1b. The distance from the conductive screen with circular aperture having d=100μm diameter to the scanned surface of the sample is z_0=75μm.

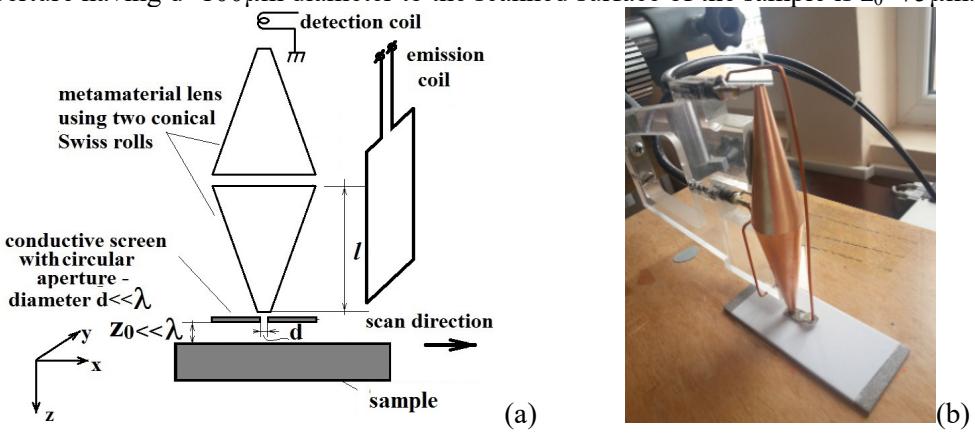

Figure 1. Sensor with metamaterial lenses: (a) principle scheme; (b) physical realization.

Electromagnetic sensors with MM lens is made using conical Swiss rolls (CSR) [19], the operation frequencies depending both by the constitutive parameters of MM lens as well as by the polarization of the incident electromagnetic field (TE_z or TM_z). The MM lens has been realized with two CSRs having a large basis face to face. This MM slab forms perfect lens [20], [21] and is focusing the electromagnetic field and also the evanescent waves. The MM lens assures the possibility to apply of electromagnetic MM in eNDE [22]. As shown in [19], the sensor with a lens realized with CSR, functioning in the range of frequencies such that μ_{eff} is maximum. Moreover, working at frequency that assures $\mu_{eff} = -1$ for the same lens, the magnetic evanescent modes can be focalized [23]. The detection principle is similar with the one of near-field electromagnetic scanning microscopy (NFESM). The functioning of the detection system can be described using Fourier optics [24], [25].

2.2.2. Equipment. NDT is a method applied to conductive materials. The principle of the experimental set-up is presented in figure 2. The EM sensor with MM lens, presented above is connected to a Network/Spectrum/Impedance Analyzer type 4395A Agilent USA.

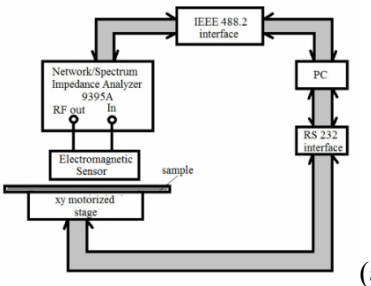

(a)

(b)

Figure 2. Experimental set-up: (a) Scheme; (b) photo.

During the measurements, the sensor was fixed and the samples is mounted on a XY displacement system, type Newmark USA that assures the displacement in plan with ±10 μm precision. That assures the scanning of sample with established steps in both directions. A PC allows the command of manipulation and measurement instruments, the data being acquired and stored automatically.

2.3. Basic principle of focused image

In order to obtain the good results of the NDT methods is necessary to obtain focused images on different planes. Let consider that the emission part of the sensor generated in material spherical waves with wave number k and let $\overline{R}$ being the position vector of the scatter. The scatter field will be [26]

$$\theta_H = ck\,\mathrm{sinc}(kR) \tag{1}$$

where c is a complex constant and $R = |\overline{R}|$. The sensor scan the surface at the constant height $z_0 \square \lambda$ and the scatter being located at depth z_1 below the surface, therefore the distance between sensor and scatter is z_1. Let U(x,y,z) be the signal delivered by the sensor and $\tilde{U}(u,v,z_0)$ its 2D Fourier transform, where u and v are spatial frequencies associated to x and y directions. We denote by $\tilde{\theta}(u,v,z)$ the 2D Fourier transform of the point spread function. The filtered and focused signal is given by the 2D Fourier transform of the convolution product of $\tilde{U}(u,v,z_0)$ by the kernel $\tilde{\theta}(u,v,z)$.

$$A(x,y,z) = \frac{1}{(2\pi)^2}\int_{-\infty}^{\infty}\int_{-\infty}^{\infty}\tilde{U}(u,v,z_0)\tilde{\theta}(u,v,z)\exp j(ux+vy)\,dudv \tag{2}$$

The image processed in this way can be obtained with

$$I(x,y) = |A(x,y,z)|^2 \tag{3}$$

3. Results and discussions

3.1. Structural parameters

Due to the porous structure of ZrO_2, comparatively with AISI 316L substrate, to obtain relevant information about the influence of yttria concentration over the adherence at support, Secondary Electrons (SE) images, as well as Backscattered Electrons (BSE) images (figure 3a and c) were taken. SEM images emphasize that the 316L steels substrate is compact, with little inclusions and/or pores between the support and the ZrO_2 layer. In this line, according to result obtained in [27] it can be observed that with the doping with yttria, the voids are larger, however their number decreases.

Using a procedure for image processing was determined that pores created about 3 up-to 12% of the analyzed layers. Pores are distributed random and nonhomogeneous. Modification of crystallite type, size and shape was not possible to determine by microscopic techniques exactly, therefore modification of crystallites will be further studied by JINR Dubna with use of techniques based on diffraction. In figure 3 b and d are presented the histograms of voids data. It can be observed that with

the doping with yttria, the voids are larger, however their number decreases. The presence of pores in material can be observed, being indifferent by the deposition methods, their difference being given only by the dimensions and density of distribution. The deformation of particles at the impact with the support material hasn't analyzed in detail, being the subject of further studies.

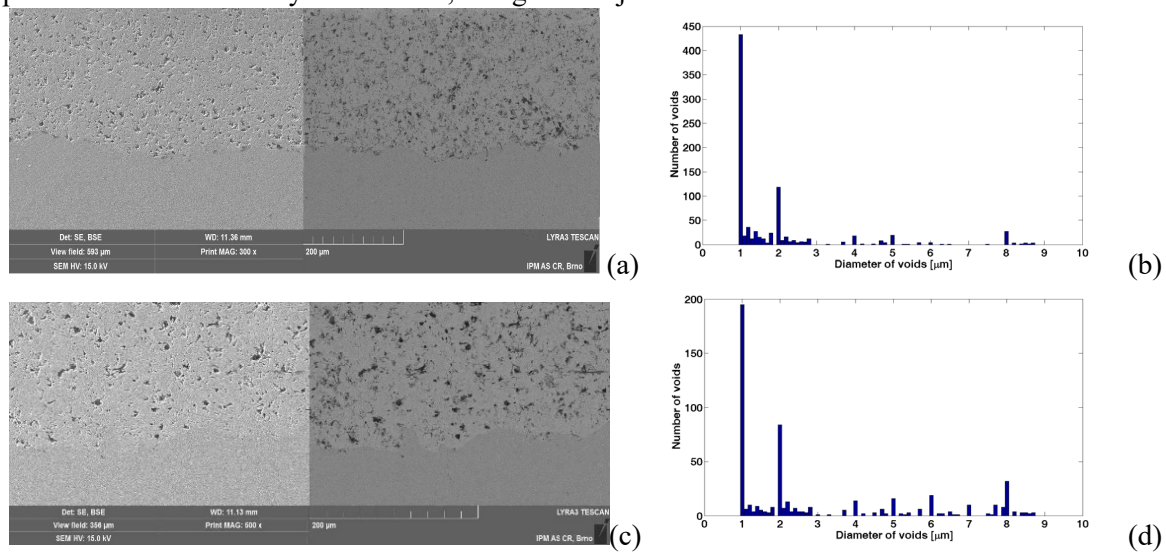

Figure 3. SEM images (left) and voids counting (right): a) and b) for specimen with 0.2 mm thick monolithic coating ZrO_2 with addition of 20 % Y_2O_3; c) and d) for specimen with sandwich coating 0.25 mm ZrO_2 with addition of 20 % Y_2O_3 and 0.005 mm Y_2O_3.

Transversal line profiles have been taken into consideration for both specimens, in order to determine the uniformity of the deposition. The profile analysis of SEM (figure 4) shows that the peaks have a constant relative mean value.

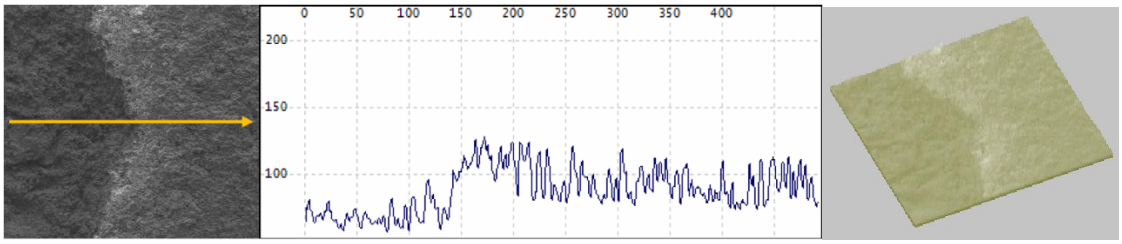

Figure 4. (a) Profile of ZrO_2 + 20 % Y_2O_3 deposition on AISI316L; (b) 3D SEM of surface.

Monolithic zirconia doped with yttria coatings having different thickness and also sandwich zirconia doped with yttria with pure yttria coating were analyzed. It was found that no visible boundary between ZrO_2 and Y_2O_3 layers of the sandwich ceramic coating can be observed using SE and BSE, therefore other techniques are needed for the detection of very thin Y_2O_3 layer. In figure 4b is presented the SEM image of the ceramic layer, in initial state without addition of Y_2O_3. Two regions are emphasized, the TBC layer ZrO_2 + 20 % Y_2O_3 and the metallic support.

In order to better characterize of the interface between support and zirconia layer, SEM and Energy Dispersive X-ray Spectroscopy (EDXS) analysis have been performed [27]. The chemical composition of the surface coating (zirconia doped with 20 % yttria) of studied samples is presented in figure 5, the presence of Zr, O, Y being emphasized.

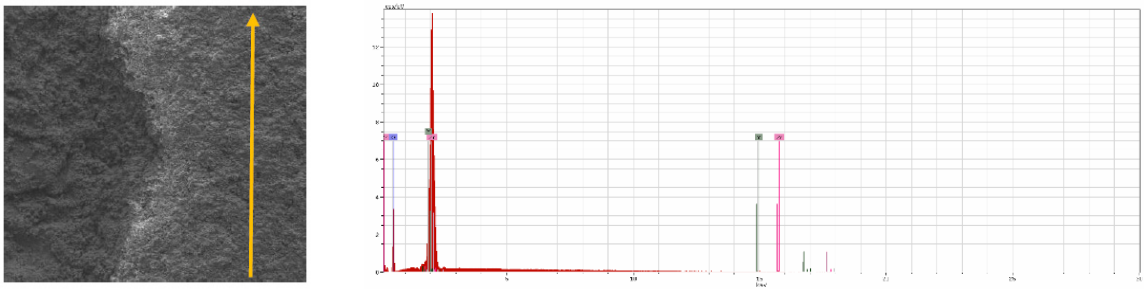

Figure 5. EDXS of specimen with 0.2 mm thick monolithic coating ZrO_2 + 20 % Y_2O_3.

3.2. Results of electromagnetic testing

The surface and bonding quality of support-layers are examined. The impedance values are affected by several parameters, as lift-off, inspection frequency, material conductivity, and the presence of inhomogeneity on or near the object surface. Ceramic zirconia top-coating is nonconductive and nonmagnetic, these create a probe lift-off effect. The sensor with MM lens has allowed the identification and estimation of the zones where the nanoparticles have created shear distortions, possible to degenerate in the damage of the coatings. The samples were placed on the displacing system, with emission coil perpendicular on the surface and on scanning direction (figure 1a).

The measurement frequency has been 105MHz. The sample were scanned on 10x10mm^2 with 200µm scanning step. In figure 6 are presented the amplitude of the voltage induced in the reception coil of the electromagnetic sensor at the scanning of the corresponding zone from the sample.)

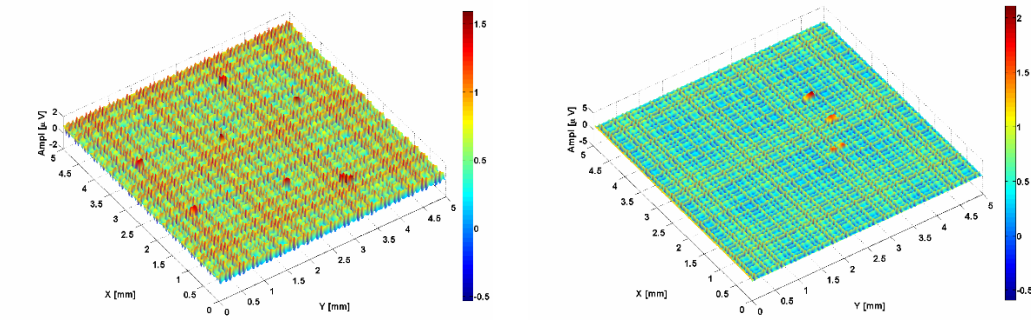

(a) (b)

Figure 6. The amplitude of the voltage induced in the reception coil of the electromagnetic transducer at the scanning of the two specimens: a) 0.2 mm thick monolithic coating ZrO_2 with addition of 20 % Y_2O_3; b) sandwich coating 0.25 mm ZrO_2 with addition of 20 %Y_2O_3 and 0.005 mm Y_2O_3.

4. Conclusions

Using a MM lens, CSR type, and following the method described above, from the zone inspected, the results allow the characterization of the surface microstructure and possible spallation/delamination at the interfaces of deposited layers. Also small roughness can be emphasized. The results of the NDT method have been confirmed by optical methods.

Further tests on a larger number of specimens with different coating aspects of the surface / number of layers are needed to establish the accuracy of the results and also the correlation between the located very small defect in size and the results of MM sensor response.

5. References

[1] Schulz U, Leyens C, Fritscher K, Peters M, Saruhan-Brings B, Lavigne O, Dorvaux J M, Poulain M, Mévrel R and Caliez M 2003 Some recent trends in research and technology of advanced thermal barrier coatings *Aerospace Science and technology* **7(1)** pp 73-80

[2] Renusch D and Schütze M 2007 Measuring and modeling the TBC damage kinetics by using acoustic emission analysis *Surface and Coatings Technology* **202(4)** pp 740-744
[3] Newaz G and Chen X 2005 Progressive damage assessment in thermal barrier coatings using thermal wave imaging technique Surface and Coatings Technology 190(1) pp 7-14
[4] Peng X and Clarke D R 2000 Piezospectroscopic analysis of interface debonding in thermal barrier coatings Journal of the *American Ceramic Society* **83(5)** pp 1165-1170
[5] www.ceramtec.com
[6] Ryshkewitz E and Richardson D W 1985 Oxide Ceramics: Physical Chemistry and Technology (Hasskell General Ceramics)
[7] Ren X and Pan W 2014 Mechanical properties of high-temperature-degraded yttria-stabilized zirconia *Acta Materialia* **69** pp 397–406
[8] Rühle M 1997 Microscopy of structural ceramics *Advanced Materials* **9(3)** pp 195-217
[9] Heuer A H, Chaim R and Lanteri V 1988 Review: Phase Transformations and Microstructural Characterization of Alloys in the System Y2O3-ZrO2 *Advances in Ceramics: Science and Technology of Zirconia III* **24** (Ohio: American Ceramics Society Westerville)
[10] Schulz U 2000 Phase Transformation in EB-PVD Yttria Partially Stabilized Zirconia Thermal Barrier Coatings during *Annealing Journal of the American Ceramic Society* **83** pp 904-910
[11] Chen W R, Wu X, Marple B R, Nagy D R and Patnaik PC 2008 TGO Growth Behaviour in TBCs with APS and HVOF Bond Coats *Surface and Coatings Technology* **202(12)** pp 2677-2683
[12] Karaoglanli A C, Altuncu E, Ozdemir I, Turk A and Ustel F 2011 Structure and durability evaluation of YSZ+ Al 2 O 3 composite TBCs with APS and HVOF bond coats under thermal cycling conditions *Surface and Coatings Technology* **205** pp S369-S373
[13] Maurel V De Bodman P and Rémy L 2011 Influence of substrate strain anisotropy in TBC system failure *Surface and Coatings Technology* **206(7)** pp 1634-1639
[14] Evaresto R A 2015 Theoretical Modelling of Inorganic Nanostructures: Symmetry and ab-initio Calculations of Nanolayers Nanotubes and Nanowires (Berlin: Springer Verlag)
[15] ACerS (American Ceramics Society, The) 2009 Progress in thermal barrier Coatings (Editor) (New Jersey: John Wiley&Sons)
[16] Feuerstein A, Knapp J, Taylor T, Ashary A, Bolcavage A and Hitchman N 2008 Technical and economical aspects of current thermal barrier coating systems for gas turbine engines by thermal spray and EBPVD: a review *Journal of Thermal Spray Technology* **17(2)** pp 199-213
[17] Chowdhury S G, Das S, Ravikumar B and De PK 2006 Twinning-induced sluggish evolution of texture during recrystallization in AISI 316L stainless steel after cold rolling *Metallurgical and Materials Transactions A* **37(8)** pp 2349-2359
[18] Matsui K, Tanaka K, Yamakawa T, Uehara M, Enomoto N and Hojo J 2007 Sintering kinetics at isothermal shrinkage: II effect of Y2O3 concentration on the initial sintering stage of fine zirconia powder *Journal of the American Ceramic Society* **90(2)** pp 443-447
[19] Grimberg R, Savin A, Steigmann R, Serghiac B and Bruma A 2011 Electromagnetic non-destructive evaluation using metamaterials *Insight-Non-Destructive Testing and Condition Monitoring* **53(3)** pp 132-137
[20] Engheta N and Ziolkowski R W eds., 2006 Metamaterials: physics and engineering explorations (John Wiley & Sons)
[21] Pendry J B 2000 Negative Refraction Makes on Perfect Lens *Physical Review Letters* **85** pp 3966-3969
[22] Grimberg R, Savin A and Steigmann R 2012 Electromagnetic imaging using evanescent waves *NDT & E International* **46** pp 70–76
[23] Grbic A, Eleftheriades GV 2003 Growing evanescent waves in negative-refractive-index transmission-line media *Applied Physics Letters* **82(12)** pp 1815-1817
[24] Born M and Wolf E 1975 Principle of Optics 5th ed (UK: Pergamon Press Oxford)

[25] Goodman J W 2005 Introduction to Fourier Optics 3rd ed (USA: Roberts & Company Englewood CO)
[26] Langenberg K J, Fischer M, Berger M and Weinfurter G 1986 Imaging performance of generalized holography *Journal of the Optical Society of America A* **3(3)** pp 329-339
[27] Faktorova D, Novy Fr, Savin A, Iftimie N, Turchenko V and Craus M L 2015 Evaluation of Zirconia coatings on some stainless steels 20th International Workshop on Electromagnetic NonDestructive Evaluation (TBP in Electromagnetic Nondestructive Evaluation (XIX), *Studies in Applied Electromagnetics and Mechanics* **41** 2016)

6. Acknowledgments

This paper is supported by Romanian Ministry of National Education under project PN-II-PCE-2012-4-0437 IDEAS.